

Structure and shaping processes within the extended atmospheres of AGB stars

M. Wittkowski¹, D. A. Boboltz², I. Karovicova¹, K. Ohnaka³, A. E. Ruiz-Velasco^{1,4}, M. Scholz^{5,6}, and A. Zijlstra⁷

¹ *ESO, Karl-Schwarzschild-Str. 2, 85748 Garching bei München, Germany*

² *US Naval Observatory, 3450 Massachusetts Avenue, NW, Washington, DC 20392-5420, USA*

³ *Max-Planck-Institut für Radioastronomie, Auf dem Hügel 69, 53121 Bonn, Germany*

⁴ *Departamento de Astronomía, Universidad de Guanajuato, Apartado Postal 144, 36000 Guanajuato, Mexico*

⁵ *Zentrum für Astronomie der Universität Heidelberg (ZAH), Institut für Theoretische Astrophysik, Albert-Ueberle-Str. 2, 69120 Heidelberg, Germany*

⁶ *Sydney Institute for Astronomy, School of Physics, University of Sydney, Sydney, NSW 2006, Australia*

⁷ *Jodrell Bank Centre for Astrophysics, School of Physics and Astronomy, University of Manchester, Manchester M13 9PL, UK*

Abstract. We present recent studies using the near-infrared instrument AMBER of the VLT Interferometer (VLTI) to investigate the structure and shaping processes within the extended atmosphere of AGB stars. Spectrally resolved near-infrared AMBER observations of the Mira variable S Ori have revealed wavelength-dependent apparent angular sizes. These data were successfully compared to dynamic model atmospheres, which predict wavelength-dependent radii because of geometrically extended molecular layers. Most recently, AMBER closure phase measurements of several AGB stars have also revealed wavelength-dependent deviations from 0/180 deg., indicating deviations from point symmetry. The variation of closure phase with wavelength indicates a complex non-spherical stratification of the extended atmosphere, and may reveal whether observed asymmetries are located near the photosphere or in the outer molecular layers. Concurrent observations of SiO masers located within the extended molecular layers provide us with additional information on the morphology, conditions, and kinematics of this shell. These observations promise to provide us with new important insights into the shaping processes at work during the AGB phase. With improved imaging capabilities at the VLTI, we expect to extend the successful story of imaging studies of planetary nebulae to the photosphere and extended outer atmosphere of AGB stars.

1. Introduction

Asymptotic Giant Branch (AGB) stars are low- and intermediate mass stars, such as our Sun, in their final phase of evolution that is driven by nuclear burning. Mass-loss becomes increasingly important toward the tip of the AGB evolution, when the “superwind” phase occurs. The superwind mass-loss reduces the convective stellar envelope until the star starts to shrink. Then the star evolves at almost constant luminosity to higher effective temperatures, passes the post-AGB phase, and becomes a planetary nebula (PN). In this phase the now hot inner star ionizes its envelope, which is a remnant of the superwind mass-loss during its AGB and post-AGB phases (e.g. Habing & Olofsson 2003).

While the mass-loss process during the AGB phase is the most important driver for the further stellar evolution toward the PN phase, the details of the mass-loss process and its connection to the structure of the extended atmospheres and the stellar pulsation are not well understood and are currently a matter of debate, in particular for oxygen-rich AGB stars (e.g. Woitke et al. 2006, Höfner & Andersen 2007).

In the past decade, imaging studies of PNe and protoplanetary nebulae (pPNe) have revealed a great diversity of morphologies. This variety of shapes of pPNe and PNe is seemingly caused by processes at the end of the AGB evolution, but the details of the shaping processes are not well understood (e.g. Balick & Frank 2002).

Interferometric techniques at optical and radio wavelengths have proven their ability to provide important observational constraints on the atmosphere and mass-loss process of AGB stars by resolving the stellar disk and the circumstellar environment (e.g. Quirrenbach et al. 1992, Reid & Menten 1997, Kembell & Diamond 1997, Perrin et al. 2004). Deviations from circular symmetry have been detected in the circumstellar environment (CSE) of AGB stars at radio as well as optical wavelengths (e.g. Reid & Menten 2007, Ragland et al. 2008).

Most recent studies using the near-infrared (AMBER) and mid-infrared (MIDI) instruments of the VLT Interferometer (VLTI) have added important information to our understanding of the pulsation and mass-loss of AGB stars thanks to their spectro-interferometric capabilities (Ohnaka et al. 2005, 2006, 2007; Wittkowski et al. 2007, 2008; Le Bouquin et al. 2009; Chiavassa et al. 2010).

Here, we describe our most recent observations of the structure and morphology of the extended atmosphere of AGB stars using the VLTI/AMBER instrument, and their implication on the mass-loss process and the onset of asymmetric shapes during the AGB evolution.

2. Observations

The first AMBER observations of an AGB star were obtained on 12 October 2007 on the Mira variable S Ori (period 414 days, Samus et al. 2009), and are described in Wittkowski et al. (2008). These observations used the low resolution mode of AMBER with a spectral resolution of ~ 35 and utilized the fringe tracker FINITO and three VLTI Auxiliary Telescopes (ATs) positioned on stations E0, G0, and H0 with ground baselines of 16 m, 32 m, and 48 m. Since then, we have obtained additional AMBER observations of the Mira variables S Col (325 d), T Col (225 d), W Vel (394 d), RW Vel (443 d), R Cnc (361 d), X Hya (301 d), and RR Aql (394 d) between September 2008 and June 2010. These observations used in addition to the low resolution mode the medium

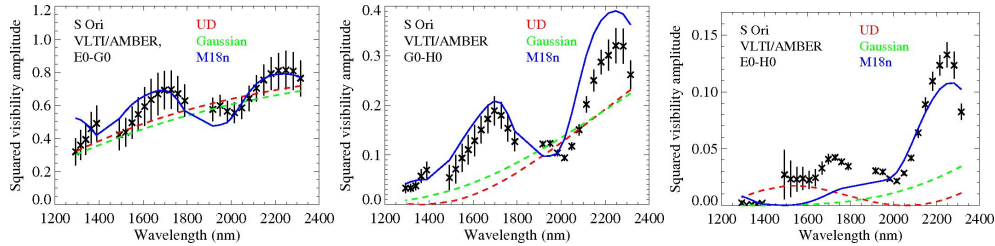


Figure 1. VLTI/AMBER visibility function of S Ori compared to simple models of a uniform disk and a Gaussian disk, as well as compared to the dynamic atmosphere model. From Wittkowski et al. (2008).

resolution modes of AMBER with a spectral resolution of ~ 1500 in the near-infrared H and K bands, and also utilized additional AT configurations. These observations will be described in detail in forthcoming papers. Some of these observations were coordinated with concurrent VLBA observations of the SiO and H₂O maser emission. In addition to Mira variables, AMBER data on OH/IR stars have been obtained in April 2008 (Ruiz Velasco et al., these proceedings).

3. Modeling

Few dynamic atmosphere models for oxygen-rich Mira stars are available. The P and M model series (Ireland et al. 2004a, 2004b) are complete self-excited dynamic model atmospheres of Mira stars designed to match the prototype oxygen-rich Mira stars α Ceti and R Leo. They have been used successfully compared to VLTI/VINCI broadband interferometric data of α Ceti and R Leo (Woodruff et al. 2004; Fedele et al. 2005). Compared to α Ceti and R Leo, our target stars have slightly different periods, masses, and radii. However, the general model results are not expected to be dramatically different for our target stars compared to α Ceti and R Leo (cf. the discussion in Wittkowski et al. 2007). As a result, the P and M model series were chosen as the currently best available option to describe Mira star atmospheres. Wittkowski et al. (2007) have added an ad-hoc radiative transfer model to these model series to describe the dust shell as observed by the mid-infrared interferometric instrument MIDI. However, at near-infrared wavelengths, the contribution of the dust shell can be neglected for our target stars. Gray et al. (2009) have combined these hydrodynamic atmosphere models with a maser propagation code in order to describe the SiO maser observations that have been coordinated for some of our target stars.

4. Results

Fig. 1 shows the AMBER visibility data of S Ori from Wittkowski et al. (2008). The visibility data of S Ori show significant wavelength-dependent features clearly deviating from uniform disk (UD) and Gaussian models of constant diameter on all three baselines. This indicates variations in the apparent angular diameter. For comparison, γ Eri, a regular M giant, was observed during the same night with the same instrument settings, and did not show such deviations from a UD curve, confirming that the features seen for S Ori are not instrumental or atmospheric effects.

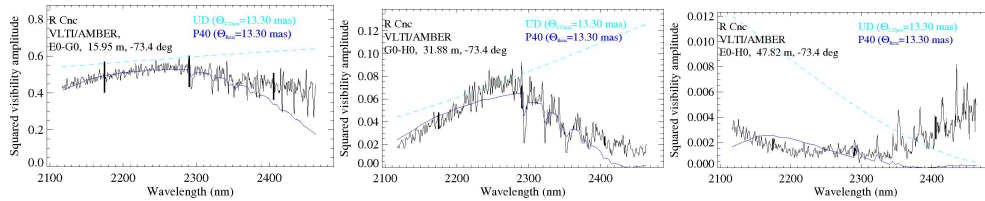


Figure 2. VLT/AMBER visibility function of R Cnc compared to a simple model of a uniform disk, as well as compared to a dynamic atmosphere model.

Model M18n provided the best formal fit to our S Ori visibility data out of the available phase and cycle combinations of the M series. The synthetic visibility values based on the M18n model compared to our AMBER observation are also indicated in Fig. 1, showing that our AMBER visibility data could be described well by the dynamic atmosphere model series. The deviations of the model visibilities from a uniform disk of constant diameter is caused by molecular layers (most importantly CO and H₂O) lying above the continuum-forming layers. At spectral channels, where the molecular opacity is low, we see a larger contribution from the photosphere, and the target appears smaller. At spectral channels where the molecular opacity is larger, we see a larger contribution from the extended atmospheric molecular layers, and the target appears larger.

In summary, our AMBER observations of S Ori generally confirmed the predictions by the M model series and we found that the observed variation of diameter with wavelength can be understood as the effect of phase-dependent water vapor and CO layers lying above the photosphere. We also concluded that more such observations on more targets and at more phases were needed to confirm and constrain the model predictions in more detail.

Since the work described in Wittkowski et al. (2008), we have obtained additional AMBER data of more targets and at more phases, as described in Sect. 2. Fig. 2 shows as an example the visibility function of the Mira variable R Cnc obtained with the medium resolution model of the AMBER instrument (spectral resolution ~ 1500). These data confirm the conclusion from Wittkowski et al. (2008) that Mira variables show wavelength-dependent angular diameters when observed with spectro-interferometric techniques that can be explained by molecular layers lying above the continuum-forming photosphere, and that are consistent with predictions by dynamic model atmospheres. In addition to these AMBER observations, Chiavassa et al. (2010) have obtained AMBER data of the very cool late-type star VX Sgr, and Ruiz Velasco et al. (these proceedings) have obtained AMBER data of three highly evolved AGB stars of OH/IR type. All these data show similar characteristics of the AMBER visibility function. The characteristic 'bumpy' AMBER visibility curves indicating the presence of molecular layers, thus seems to be a common feature of evolved oxygen-rich stars.

5. Shaping processes

Fig. 3 shows the AMBER closure phase measurement corresponding to the visibility curves of Fig. 2. The interferometric closure phase is a measure of the point symmetry of a source. Values of 0° and 180° indicate point symmetry, other values deviations from point symmetry. R Cnc shows closure phase values that are significantly different

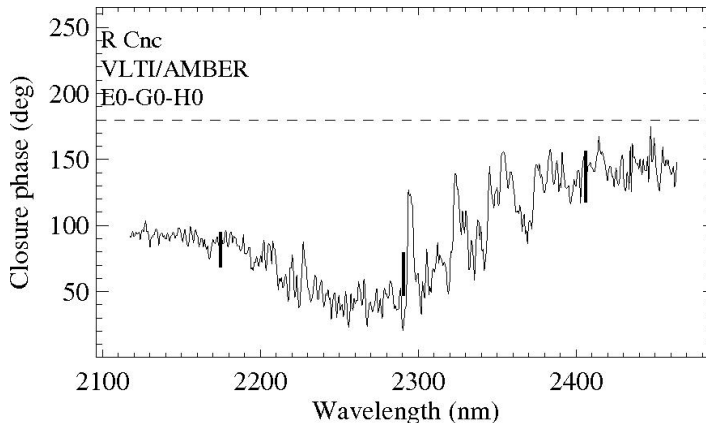


Figure 3. VLT/AMBER closure phase of R Cnc.

from 0° and 180° , thus indicate a significant deviation from point symmetry. The R Cnc closure phases vary with wavelength. At wavelengths around $2.25\mu\text{m}$, where the visibility values show a maximum corresponding to a small angular diameter, the closure phase shows values of about 40° . Shortward of $2.25\mu\text{m}$, where the visibility decreases and where the water vapor opacity becomes larger, the closure phase increases to 90° . Longward of $2.25\mu\text{m}$, where the visibility decreases both due to CO and water vapor, the closure phase increases to 150° , with closure phase peaks marking the peaks of the CO bandheads. A similar characteristic signal of the closure phases are seen for other targets of our sample.

The interpretation of the closure phase measurements is work in progress. They might indicate a complex non-spherical stratification of the photosphere and extended atmosphere, and may reveal whether observed asymmetries are located near the photosphere or in the outer molecular layers. These observations thus promise to lead to new insights into the shaping processes at work during the AGB phase. As an example, the detection of photospheric convection cells and corresponding clumps in the molecular layer that have characteristics as those predicted by 3D atmosphere models (e.g. Freytag & Höfner 2008) would point to a process of large-scale photospheric convection. Random clumps in the molecular shell may point to highly temporally and also spatially variable chaotic mass ejections caused by perturbations in the oscillations (Icke et al. 1992) or by magnetic fields (e.g. Suzuki 2007).

6. Summary

AMBER spectro-interferometry shows wavelength-dependent apparent sizes of AGB stars, including Mira variables and OH/IR stars. These observations are generally consistent with dynamic model atmosphere predictions that include molecular layers, in the infrared most importantly CO and H₂O, lying above the continuum-forming photosphere. AMBER closure phase measurements of a sample of resolved Mira variables indicate deviations from point symmetry. A characteristic wavelength dependence of the closure phase values indicates a complex non-spherical stratification of the extended atmosphere. A detailed interpretation of these measurements is needed, and may reveal whether asymmetric structures originate at the photosphere or at more extended layers,

and how they develop from smaller to larger scales. Advanced imaging capabilities with the VLTI thanks to improved baseline configurations and 2nd generation instruments combining a larger number of beams will allow us to obtain model independent images of the extended atmospheres of AGB stars. We are thus at a turning point in the history of knowledge of AGB stars, where imaging studies can be extended from pPNe and PNe to layers of AGB stars at the photosphere and at molecular layers close to the photosphere, and thus reveal the shaping processes at work during the AGB phase.

References

- Balick, B., & Frank, A. 2002, *ARA&A*, 40, 439
Chiavassa, A., Lacour, S., Millour, F., et al. 2010, *A&A*, 511, 51
Fedele, D., Wittkowski, M., Paresce, F., et al. 2005, *A&A*, 431, 1019
Freytag, B., & Höfner, S. 2008, *A&A*, 483, 571
Gray, M. D., Wittkowski, M., Scholz, M., et al. 2009, *MNRAS*, 394, 51
Habing, H. J., & Olofsson, H. 2003, *Asymptotic giant branch stars*, by Harm J. Habing and Hans Olofsson. *Astronomy and Astrophysics Library*, New York, Berlin: Springer, 2003,
Höfner, S., & Andersen, A. C. 2007, *A&A*, 465, L39
Icke, V., Frank, A., & Heske, A. 1992, *A&A*, 258, 341
Ireland, M. J., Scholz, M., & Wood, P. R. 2004a, *MNRAS*, 352, 318
Ireland, M. J., Scholz, M., Tuthill, P. G., & Wood, P. R. 2004b, *MNRAS*, 355, 444
Kemball, A. J., & Diamond, P. J. 1997, *ApJ*, 481, L111
Le Bouquin, J.-B., Lacour, S., Renard, S., et al. 2009, *A&A*, 496, L1
Ohnaka, K., Bergeat, J., Driebe, T., et al. 2005, *A&A*, 429, 1057
Ohnaka, K., Driebe, T., Hofmann, K.-H., et al. 2006, *A&A*, 445, 1015
Ohnaka, K., Driebe, T., Weigelt, G., & Wittkowski, M. 2007, *A&A*, 466, 1099
Perrin, G., Ridgway, S. T., Mennesson, B., et al. 2004, *A&A*, 426, 279
Quirrenbach, A., Mozurkewich, D., Armstrong, J. T., Johnston, K. J., Colavita, M. M., & Shao, M. 1992, *A&A*, 259, L19
Ragland, S., Le Coroller, H., Pluzhnik, E., et al. 2008, *ApJ*, 679, 746
Reid, M. J., & Menten, K. M. 1997, *ApJ*, 476, 327
Reid, M., & Menten, K. 2007, *ApJ*, 671, 2068
Samus, N. N., Durlevich, O. V., et al. 2009, *VizieR Online Data Catalog*, 2025
Suzuki, T. K. 2007, *ApJ*, 659, 1592
Wittkowski, M., Boboltz, D. A., Ohnaka, K., et al. 2007, *A&A*, 470, 191
Wittkowski, M., Boboltz, D. A., Driebe, T., et al. 2008, *A&A*, 479, L21
Woitke, P. 2006, *A&A*, 460, L9
Woodruff, H. C., Eberhardt, M., Driebe, T., et al. 2004, *A&A*, 421, 703